Journal of Materials Processing Tech. 302 (2022) 117483

Contents lists available at ScienceDirect

Journal of Materials Processing Tech.

journal homepage: www.elsevier.com/locate/jmatprotec

Experimental analysis of subsurface integrity during fine turning of OFE copper for radiofrequency cavity manufacturing

A. Camelin [a,b,c], P. Naisson [a,*], G. Poulachon [b], A. D'Acunto [c], S. Atieh [a]

[a] CERN Engineering Department, Mechanical & Materials Engineering Group, CERN - 1211 Geneva 23, Switzerland
[b] Arts et Metiers Institute of Technology, LaBoMaP, 71250, Cluny, France
[c] Laboratoire d'Etude des Microstructures et de Mécanique des Matériaux, Ile de Saulcy, 57045, Metz, France

ARTICLE INFO

Associate Editor: Erhan Budak

Keywords:
Machining
Surface integrity
Radio frequency cavity
OFE copper
Microstructure
EBSD
FIB

ABSTRACT

Machining oxygen-free electronic (OFE) copper could be challenging but is not widely studied because few industrial or critical components requires to master the machined sub-surface characteristics. CERN radio frequency cavities are one of the applications, especially because the turned surface is not the functional one of the final products. The niobium coating post process, which gives superconductive properties to the cavity, largely depends on the machined surface characteristics. The present study relies on an experimental approach of the cutting process, through thermal and mechanical probing of high precision, pollution free, turning. Cutting forces and thermal load on the tool are detailed for finish turning. The critical uncut chip thickness, defined at macroscale as the limit between cutting and ploughing behavior, is also a frontier at microscale. Consequently, surface integrity is evaluated by advance microstructural analysis (EBSD and FIB), imposed by the thinness of the affected layer. Grain recrystallization appears in the first 0.6 micrometers below the surface and deformed grains are observed up to 4 micrometers for cutting regime, while the thickness of the layers is three time larger in case of ploughing regime. Hence surface integrity of OFE copper finish turning is characterized and optimal cutting conditions are defined. The research shows that simple cutting tests can quickly narrow down to optimal cutting condition, which are then confirmed through metallurgical analysis, even in the edge case of pure OFE copper, hence relevant to other material.

1. Introduction

In addition to the Large Hadron Collider impact on fundamental nuclear physics, CERN houses numerous so-called fixed-target experiments. The HIE-ISOLDE experiment aims to increase the energy and efficiency of the ISOLDE nuclear facility by upgrading its accelerating components, through thirty-two 40 MV superconducting quarter-wave resonators (Fraser et al., 2017).

For these newly designed cavities, the niobium-on-copper technology was selected. It implies the use of magnetron sputtering of a thin (2–10 micrometers) layer of pure RRR300 Niobium on an high purity copper substrate obtained after machining process as shown on Fig. 1 (Sublet et al., 2014). It has been previously established that the quality of the copper substrate (structure, homogeneity, porosity, mechanical and electrical characteristics) is strongly connected to the surface texture and overall surface integrity. Furthermore, only cutting processes, such as turning or milling, are acceptable to produce radiofrequency (RF) required surface characteristics, whereas abrasive processes, such as grinding or lapping, are banned, because of risks of debris or dust partial sticking, even if better surface finish can be obtained (Ghosh et al., 2021). Hence, superfinishing machining operation must be used, especially high precision turning. Given the size of the inner (>Ø90 mm) or outer conductor (Ø 320 mm, wall thickness > 15 mm), for an approximate weight of 185 kg, compared to the scale of the studies in the surface and subsurface (<0.5 mm), the geometry of the part will be considered without influence.

Surface and subsurface characteristics are linked to the machining process parameters, such as tool type, cutting data, or lubrication modes (Bellows and Tishler, 1970). For finishing operations, the first 200 micrometers underneath the surface is a volume of intense material transformations, such as grain refinement (Herbert et al., 2012), (dynamic) recrystallization (Denguir et al., 2014), oxidation and multiple other phenomena linked to mechanical and thermal loads applied by the cutting edge on the finished surface (la Monaca et al., 2021). Thus,

* Corresponding author.
E-mail address: pierre.naisson@cern.ch (P. Naisson).

https://doi.org/10.1016/j.jmatprotec.2021.117483
Received 1 October 2021; Received in revised form 21 December 2021; Accepted 26 December 2021
Available online 28 December 2021

mastering the cutting process is the way to ensure proper surface functionality (AFNOR, 1997).

It is even more important for RF application as the surface dependent fields (magnetic and electric) are known to appear within the first few hundreds of nanometers below the (Sublet et al., 2014). Fig. 2 illustrates the manufacturing process creating the multiple layers, the niobium coating is the final operation, performed on an affected material which may differ from the base material, depending on the cutting process.

In particular, the uncut chip thickness, the chip area and the cutting speed are key parameters for subsurface damage control (Herbert et al., 2012). Moreover, in the special case of superfinishing operation, the roughness criteria lead to a reduction of chip load to a condition where the cutting process is disturbed by the ploughing effect of the tool edge radius (Chae et al., 2006). Below a critic uncut chip thickness h_{crit}, the cutting phenomenon disappears, changing to indentation or sliding process (Rech, 2008), and dramatically modifying the mechanical and thermal loads of the finished surface and the primary shear zone (Ni and Alpas, 2003). Some geometrical considerations can be discussed to estimate h_{crit} value (Denkena and Köhler, 2010), consequently controlling this effect.

Another aspect concerns the heat generated by the friction between the tool and the work material. This friction coefficient and heat partition ratio depend on work material, tool material (Naisson et al., 2013), coating and cutting fluid media (Mondelin et al., 2011). For superfinishing of copper, and to prevent chemical pollution, the micro pulverization techniques (minimum quantity lubrication MQL) is often coupled with ethanol-based fluid. With the selected parameters, it is possible to obtain very fine droplets of fluid dispersed in a large volume of air, leading to a lower friction coefficient and heat flow, hence reducing the load on the finished surface (Cabanettes et al., 2017). Since the condition of lubrication affects the thermal condition at the tool-surface interface, it changes the heat equilibrium, reducing the heat flow in the tool (Klocke and Eisenblätter, 1997), but with also an effect on the part itself.

In case of OFE copper, the metallurgical and mechanical characteristics emphasis the sublayer damage toward a grain refinement up to 50 to 200-nanometers grain size (Ni and Alpas, 2003) and dynamic recrystallization (Liu et al., 2015). Recent advances in numerical modelling have led to a finer understanding of the intertwined physics occurring in the subsurface layer (Gravier, 2009). Especially the depth of the affected layer is sensitive to original microstructure and friction at the contact zone between the tool and the material (Atmani et al., 2015). The friction phenomenon is of major influence and both modelling (Kermouche et al., 2016) and experimental setup parameters (Denguir et al., 2017) show an affected layer between 20 μm and 80 μm. The main driving parameter of the affected layer seems to be the cutting speed, and by extension the thermal cycle which is seen by the material (Lin et al., 1997). It has been also demonstrated that the dynamic recrystallization and the grain refinement is linked to dislocation density (Bissey-Breton et al., 2011).

In the HIE-ISOLDE cavity manufacturing scheme, a chemical etching treatment is carried out to remove between 15 μm–40 μm of the surface before the niobium coating (Sublet et al., 2014). This is made to prevent any contamination of the layer from the bulk material. Hence, depending on the cutting configuration, a variety of grain morphology may appear and leads to coating issues such as peeling, cracks or misorientation. The present study is focused on defining the actual status of the subsurface layer produced by CERN machining conditions. Especially, the emphasis will be put on the identification of the thermomechanical loads induced by cutting, especially in the case of ploughing configuration. Forces and temperature inside the cutting tool will be measured. All the tests will be carried out on OFE copper, cut with uncoated tungsten carbide tools, with MQL alcohol lubrication method. The microstructure is characterized through TEM (Transmission Electron Microscopy), FIB (Focused Ion Beam) and EBSD (Electron Back Scatter Diffraction) methods to identify the affected layers and their morphology. Finally, the machining process to obtain OFE copper cavity in case of super finish turning will be qualified.

2. Machinability of OFE copper under alcohol micro lubrication

2.1. Copper machinability issue

Machining of copper is not widely studied because it is often compared to aluminum alloy in term of machinability. Indeed, copper is not hard (60 HBS 20 kgf, 2 mm ball) (Kupferinstitut, 2016), with yield

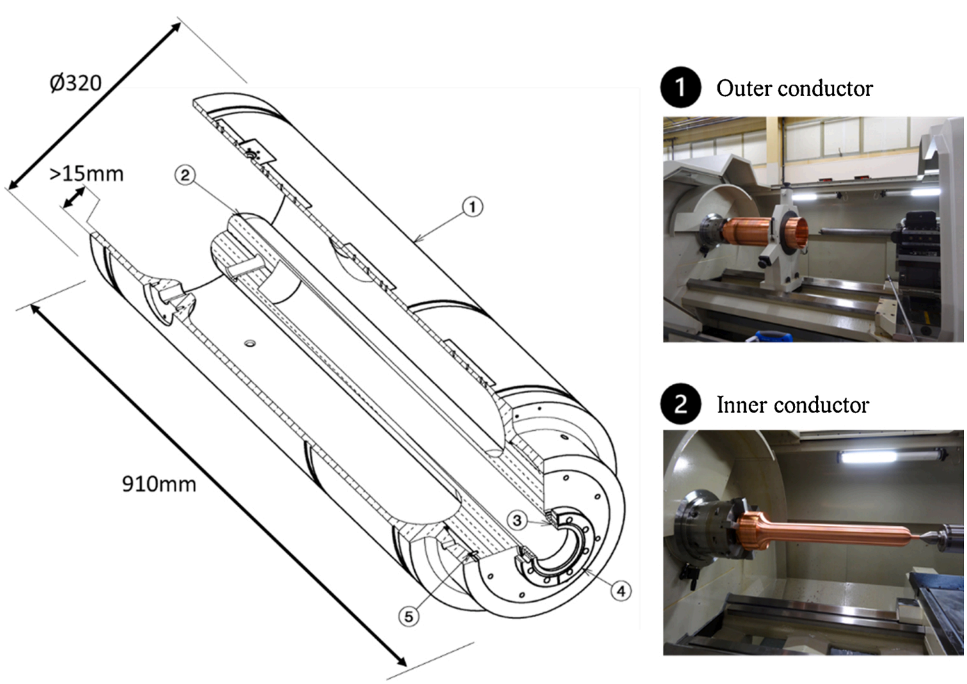

Fig. 1. ISOLDE ¾ view cross-section, outer and inner conductor. The two part are then assembled through shrink fit and electron beam welding for structural and electrical integrity (Sublet et al., 2014).

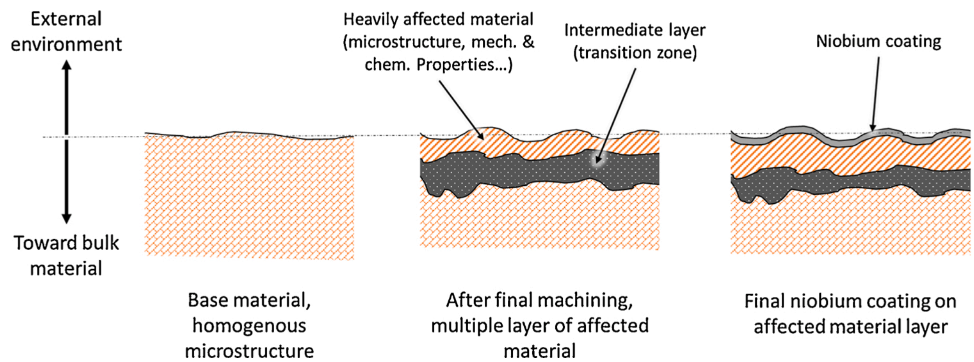

Fig. 2. Illustration of the manufacturing process and the created layers on the base material.

strength limited to around 200 N/mm^2 for the half-hard oxygen-free electronic (Cu-OFE) (CERN, 2015). But, because of its purity (99.99 % of copper) and forging process, the microstructure has a homogenous microstructure, showing few dislocations, lattice disturbances or local disorientations. The high thermal conductivity (around 400 W/m.K) induces quick and large temperature rise in the part. The tensile strength decreases below 100 N/mm^2 over 600 °C. The material becomes very soft, sticks to the tool, and creates a built-up edge. The melting temperature is 1083 °C. This soft mechanical characteristic prevents a spontaneous chip breaking, which are thus often long and intertwined as shown in Fig. 3.

2.2. Experimental setup

For radiofrequency equipment produced and used at CERN, only cutting processes are allowed to minimize the risks of virtual leaks or dust trapping inside the material. Also, the cutting fluid may cause corrosion or other metallurgical surface modification that may damage the functional surface.

Hence, it implies sharp cutting tools and cutting conditions that are closed to the machinability limits. As a second constraint, selected cutting fluid is a mix of ethyl alcohol C_2H_5OH with 3% of acetone. The alcohol machining is a standard technique when it comes to copper finishing operation, for high surface quality, as it prevents creation of corrosion or chemical contamination of the surface. This leads to very low viscosity, high volatility, hence poor lubrication but rather good cooling effect due to rapid evaporation. It is combined with micro pulverization (MQL) technique to obtain an aerosol of air and alcohol droplets. The MQL with straight oil has an intermediate performance between dry machining and flooding techniques as shown by (Bissey-Breton et al., 2011; Germain et al., 2010). But the combination of MQL, OFE copper and precision finishing turning is rarely studied since it implies antinomic machining behavior.

The selected method to compare macroscopic parameter is based on the tool material pair (TMP) method defined by AFNOR standard (AFNOR, 1997). This method is also used in other comparable studies (Bissey-Breton et al., 2011; Germain et al., 2010) and will serve as a reference. The input variables are the cutting conditions, cutting speed V_c, feed per revolution f and depth of cut a_p. The tool used at CERN for this application is a Korloy designated VCGT160404 AR H01, uncoated tungsten carbide inserts, with high rake angle of 18 ° and sharp cutting edge, with an edge radius r_β of 9 µm, controlled for each insert by Alicona system. The tool is mounted on a SVJBL 2020 K tool holder, with a major cutting-edge angle K_r of 93 °. The work material is 3D forged, half-hard C10100 OFE copper, with a maximal grain size of 90 µm (Sgobba, 2006). The cutting tests are carried out on a CNC two-axis lathe SOMAB T500, on which a Kistler 9121 dynamometer is mounted as illustrated in Fig. 4. A Kistler 5019B charge amplifier collects the signal and is transmitted to the computer with Dasylab software for recording the cutting process. The three main forces (cutting force, feed force and passive force) are recorded with a 1000 Hz sampling frequency.

The tool material pair method relies on the specific cutting pressure K_c as defined by the ratio of cutting force over the chip section $K_c = F_c/(a_p.f)$. The second parameter concerns the surface roughness R_a or R_t. Also, an equivalent uncut chip thickness h_{eq} will be calculated following (Denkena and Köhler, 2010). It is then compared to the h_{crit} value which is five-time the tool edge radius, according to (Germain et al., 2010), $h_{crit} = 5 \text{ x } r_\beta = 0.040$ mm, in this application.

$$h_{eq} = \frac{A_d}{l_{eq}} = \frac{\alpha_p \times f - \frac{1}{3} \times f \cdot \left(r_\varepsilon - \frac{\sqrt{4 \cdot r_\varepsilon^2 - f^2}}{2} \right)}{r_\varepsilon \times \left(\kappa_r + \sin^{-1} \frac{f}{2.r_\varepsilon} \right) + \sin \kappa_r \times \left(\alpha_p - r_\varepsilon (1 - \cos \kappa_{r.}) \right)}$$

Equation 1: Equivalent uncut chip thickness, adapted from (Denkena and Köhler, 2010)

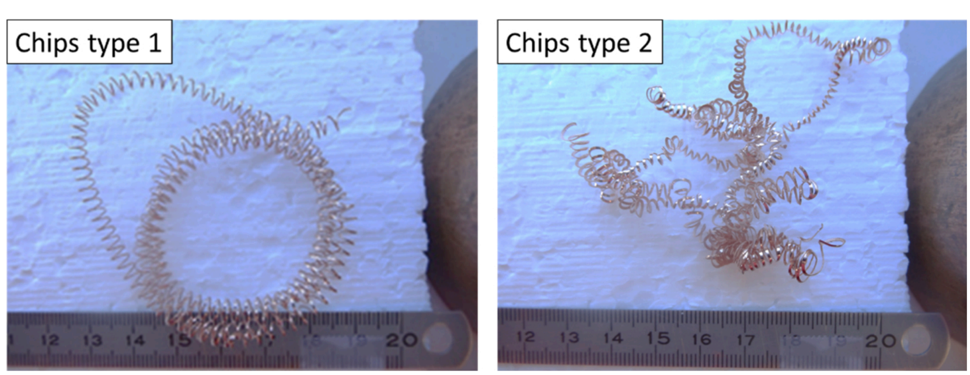

Fig. 3. Chip morphology of finish turning of copper, MQL alcohol. Chips type 1: $V_c = 160$ m/min, f = 0.05 mm/rev, $a_p = 0.3$ mm. Chips type 2: $V_c = 60$ m/min, f = 0.3 mm/rev, $a_p = 0.05$ mm.

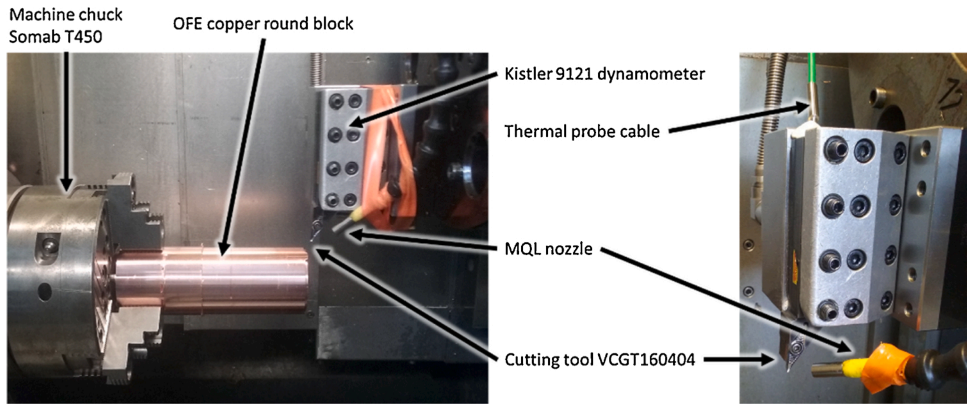

Fig. 4. Experimental setup for force and temperature measurement during turning operation of OFE copper.

For small depth of cut regarding the tool nose radius, the chip is only formed in the nose region of the tool, hence the cross-section depends mainly on feed, nose radius and depth of cut, as shown on Fig. 5.

3. Mechanical load induced by turning of OFE copper

The cutting conditions have been chosen according to actual CERN workshop practices. It should be pointed out these parameters might not be the most productive but allow reliable and consistent RF results over a wide range of cavity shape machining. Nevertheless, a window of cutting conditions is explored to identify boundaries of copper machining under fine finishing under alcohol lubrication.

The cutting speed has a limited impact on the specific cutting force, within 10 % of the mean value. As a result, cutting speed will be kept at its setting to the constant value of 120 m/min. The first raw measurements visible on Fig. 6 shows, as expected, low cutting forces, ranging from 6 to 250 N. Cutting force increases as either feed or depth of cut increase.

The same behavior could be measured for both feed and passive force as shown in Fig. 7, with special remarks on the almost negligible passive force in case of low feed rate. This has also been demonstrated by Germain et al., 2010 and is linked to no cutting or ploughing effect. In this case, the alcohol-based micro pulverization shows no fundamental difference compared to an oil-based solution, especially in the pressure contact at the rake and flank face.

Hence, the evolution of the specific cutting force versus equivalent uncut chip thickness shows two modes of operation as pointed on Fig. 8. The border between both regimes is determined through the Tool Material Pair method (AFNOR, 1997). In case of low depth of cut, no feed permits to cross the theoretical h_{crit}, leading to non-stable behavior

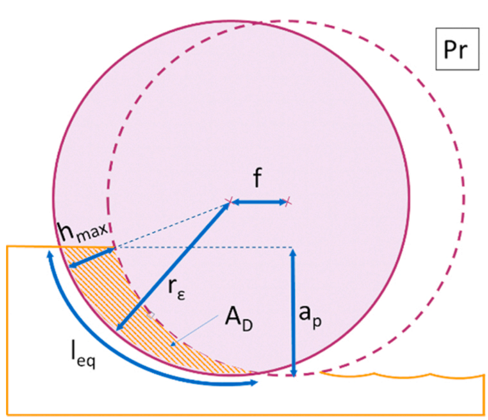

Fig. 5. Cross-section of the cutting zone, adapted from (Campocasso et al., 2015; Denkena and Köhler, 2010; Germain et al., 2010).

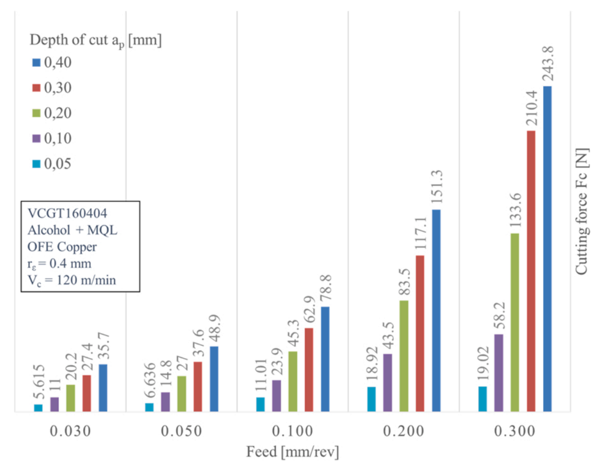

Fig. 6. Evolution of measured cutting force versus depth of cut and feed rate.

(depth of cut lower than 0.1 mm). For a greater depth of cut, a stable condition could be found for h_{eq} bigger than 0.036 mm (referred to as h_{eq}*(mini))*, close to the theoretical value of 0.040 mm. For a depth of cut higher than 0.2 mm, specific cutting force increase for an uncut chip thickness higher than 0.075 mm. This must be interpreted as an upper limit cutting conditions, or maximal stress saturation, as described in the Tool Material Pair method.

Considering the minimal equivalent chip thickness, the minimal roughness Ra which can be obtained is 0.45 μm as plotted on Fig. 9. This is only achievable by depth of cut larger than 0.3 mm. Hence the depth of cut should be chosen

It appears on Fig. 10 a chip cross-section over 0.020 mm^2 corresponding to a stabilized specific cutting force and is encountered for an equivalent uncut chip thickness higher than the h_{eq}*(mini)*. This confirms the strong effect of chip load on machining stability in terms of energy equilibrium.

Finally, the mechanical behavior of the turning operation is barely defined by the macroscopic parameter (cutting condition). In the case of a finishing operation, a local analysis must be conducted, and the critical uncut chip thickness reveals a strong role. Furthermore, chip cross-section seems to describe better the energetic stability of the process at mesoscale analysis, while cutting speed has limited effect.

4. Thermal behavior of OFE copper cutting in superfinishing turning under MQL lubrication with alcohol

The evaluation of the thermo-mechanical flow induced by the finishing operation is key to understand the structural modification of the material near the surface. Most of the energy induced by the mechanical

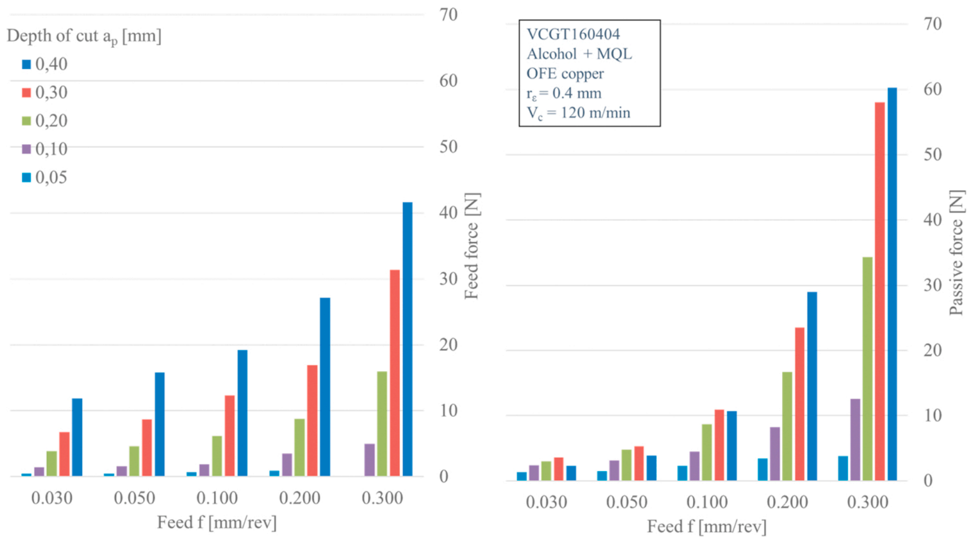

Fig. 7. Feed and passive forces evolution.

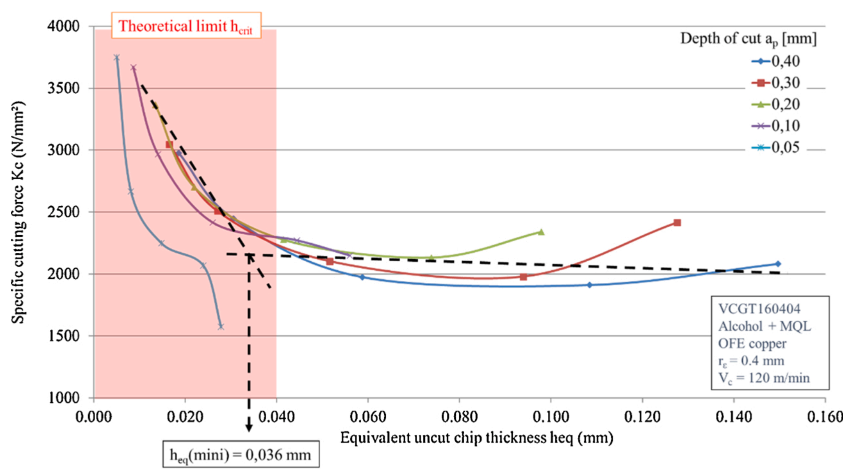

Fig. 8. Specific cutting pressure as a function of equivalent uncut chip thickness.

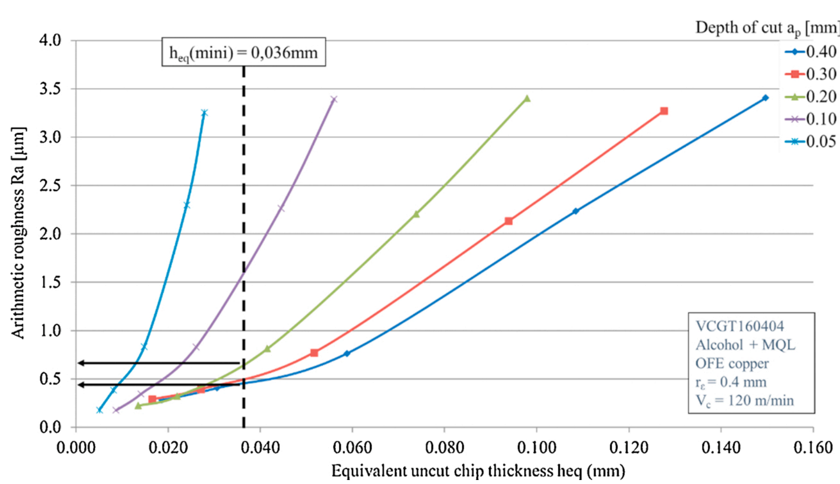

Fig. 9. Influence of h_{eq} on arithmetic roughness Ra.

load in the cutting area is turned into heat during the cutting process. Changing lubrication should not influence the heat repartition between the tool and work material as thermal balance is not impacted by a modification of the lubrication (Mondelin et al., 2011). But MQL alcohol lubrication could modify the heat equilibrium induced by the mechanical loading in the cutting area (produced by friction). To evaluate the

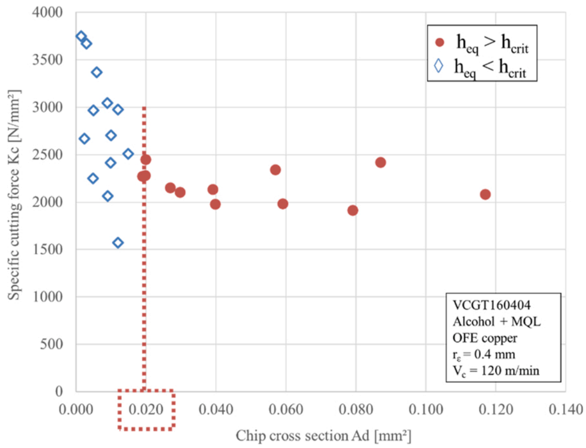

Fig. 10. Correlation between specific cutting pressure and chip cross-section.

thermal flow, a thermal evaluation of the heat output to the tool has been designed. It must be noticed that this measurement, while it is relevant for tool thermal status, can only be taken as an indication in the scope of machined surface characteristics, by pointing out macroscopic effect due to thermal balance modification. It was decided to use an insulated thermocouple, type 12, material reference K (Chromel-Alumel), with simple PVC insulation (2I 3P2L), 0.5 mm sheath diameter: reference 12-K-150-118-0.5-2l-3P2L from the supplier TCSA. As shown in Fig. 11, the thermocouple is located 0.5 mm under the rake face, and 1.5 mm away from the tip of the tool, considering the shallow tip angle (V shaped insert) and the need of keeping enough insert material to support the cutting forces.

The measured cutting forces and the thermal conductivity of OFE copper suggest a temperature range relatively low. Also, the temperature measurements are carried out from the tool perspective, at a relatively large distance for the heat generation point and does not give direct information about the actual tool tip temperature. Hence the temperature measurement must be considered as a delayed observer for the cutting process. As shown in Fig. 12, each turning operations were carried out without interruption and over a long period (>140 s) to observe a steady-state regime of cutting temperature T_{cut}. Indeed, before any cutting process and before the thermal stabilization, the temperature drops at a lower value T_{init} than the initial one T_{amb}. This is the effect of the beginning of the lubrication. For the following studies, the cutting temperature is defined as the average temperature measured during the permanent regime of the cutting process.

The location of the thermocouple, the quality of the interface are all unknown factors increasing uncertainty. Hence ΔT (evolution of the temperature in the tool) will be used as representative heat input to the tool, and defined as:

$$\Delta T = \text{Tcut} - \text{Tinit}$$

Equation 2: definition of the relative cutting temperature

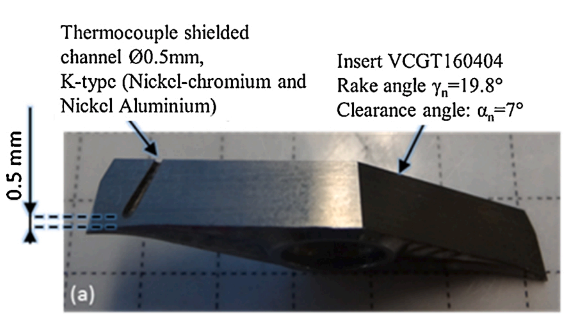

Fig. 11. Cross-section of the thermocouple location in the turning insert.

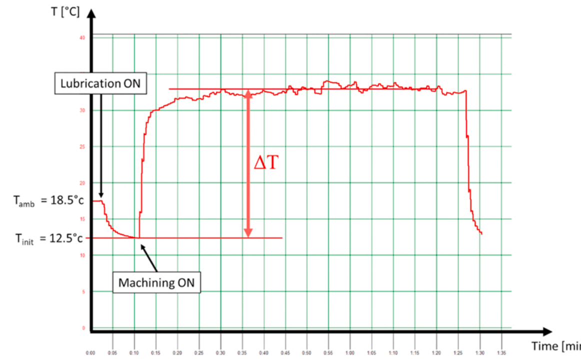

Fig. 12. Temperature evolution during the complete cutting process.

Fig. 13 shows the results of temperature measurements by varying the chip cross-section A_D. The test has been designed to highlight the influence of the critical uncut chip thickness h_{crit} defined in §1. As the cross-section increases, the temperature increases independently if the equivalent uncut chip thickness h_{eq} is higher or smaller than h_{crit}, with a linear dependency to chip cross section. No threshold can be identified for the thermal behavior.

At fixed feed rate and depth of cut and by varying cutting speed V_c from 80 to 400 m/min, as shown in Fig. 14, the temperature behavior shows a linear increase of ΔT until $V_c = 300$ m/min. Over this value, the temperature in the tool is subjected to a saturation effect and is stabilized between ΔT = 31.0 °C–32.3 °C. In the case of superfinishing conditions, cutting speed has a major influence on the cutting temperature.

Hence, the chip cross-section variation has the greatest influence on the measured temperature, if the steady-state regime is achieved, for a cutting speed higher than 300 m/min. For the following step, cutting speed is fixed at 160 m/min. This value corresponds to the production condition and permits to limit cutting speed influence on the following tests. In this case, and as for mechanical stresses, the chip cross-section is the key parameter.

Thus, during finishing operations, the tool temperature does not reach over 35 °C. It implies that the heat sources, the friction, and the shear processes, have a maximal throughput which can be handled by the coolant and the conduction to the material (through uncut chip section and finished surface). Hence, more than the heat flux value, it is the heat flux distribution, driven by the chip cross-section, that would influence most of the surface integrity, as shown by (Valiorgue et al., 2012).

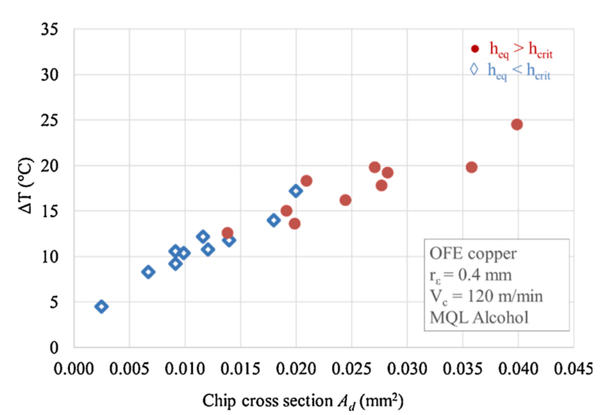

Fig. 13. Evolution of cutting temperature versus the chip cross-section.

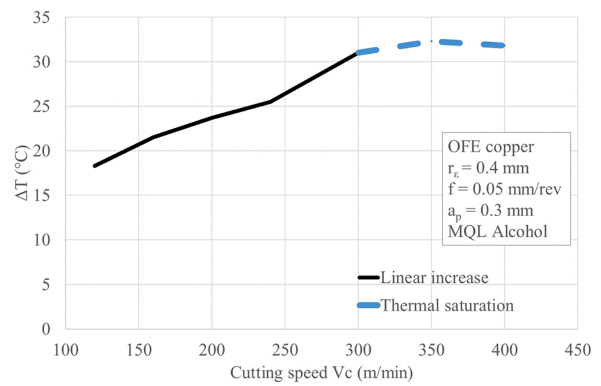

Fig. 14. Evolution of the cutting temperature versus the cutting speed.

5. Comparison of two surfaces turned in superfinishing conditions inside and outside the stable domain

Variations in machining conditions imply a modification of the thermo-mechanical phenomena. By fixing the cutting speed V_c and chip cross-section, it is possible to produce different samples and discriminate the effect of the thermo-mechanical flow on the turned sub-surface, aiming to minimize the affected layer thickness. To analyze the impact of the mechanical flow on surface integrity, two samples presented in Table 1, were produced. Therefore, interest is to find a method and characterization criteria to highlight the impact of the thermo-mechanical flow on the surface integrity under the turned surface.

As a first approach, metallurgical microscopy is used, as shown on Fig. 15. The original microstructure of the OFE copper is exposed, and the periodic waves at the top correspond to the roughness induce by the tool tip. No major evolution is visible, but a thin layer of around 10 µm seems to appear under the surface. Standard optical methods are not of help in this case.

For the RF application, the affected layers have a huge impact on the effectiveness of the cavity. As demonstrated, superfinishing turning under alcohol lubrication induces low thermo-mechanical load. However, after the finishing cutting process, the evolution of the surface sub-structure evolves in the material (Mondelin et al., 2013). And in case of pure copper, a high thermo-mechanical solicitation (Rech, 2008) provides an ultrafine microstructure composed of nano-grain induced by the activation of dynamic recrystallization. In turning operation of pure copper, this severe grain refinement has been predicted (Atmani et al., 2015) and observed (Ni and Alpas, 2003) in chips formation. Through TEM analysis a microstructure composed of elongated dislocations cell structures and grain refinement with equiaxial grains about 220 nm diameter has been shown. A grain refinement between 150 nm and 300 nm diameter is expected close to the surface. The total thickness of the affected layer A_t can be predicted with the roughness parameter R_z, according to (Bissey-Breton et al., 2011).

$$A_t\ (\mu m) = 1.36.R_Z(\mu m) + 1.03$$

Equation 3 : Roughness parameter R_z, according to (Bissey-Breton et al., 2011)

Table 1
Summary of the affected layer thickness for the two samples of the study and comparison with (Bissey-Breton et al., 2011).

	Production parameters			Measurement	Prediction (Bissey-Breton et al., 2011)
	f (mm/rev)	a_p (mm)	V_c (m/min)	Rz-measured (µm)	At (µm)
C_{prod}	0.05	0.3	160	0,8	3,2
$C_{Ploughing}$	0.3	0.05	160	16,4	23,3

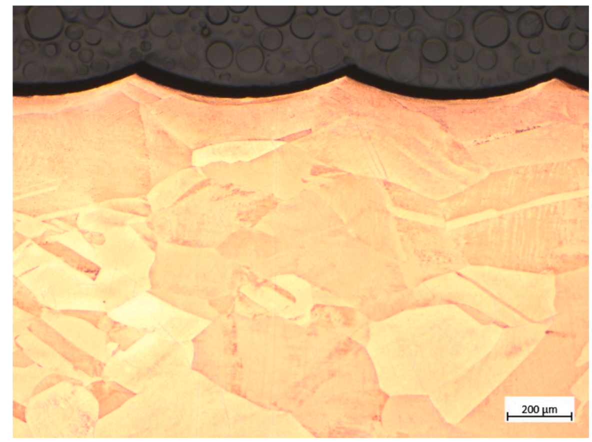

Fig. 15. Microscopic longitudinal cross section, C_{prod} cutting condition (see Table 1).

The following analysis aims to evaluate the impact of the thermo-mechanical loading on the thickness of these affected layers. In line with this objective, two different turning conditions, chosen according to the presented results, are produced for analysis: industrial conditions C_{prod} and ploughing conditions $C_{ploughing}$. These two samples present the same chip cross-section, same arithmetic roughness, but an equivalent uncut chip thickness under and over the h_{crit}. The two sets of cutting condition have been chosen to expose the influence of heat or mechanical load over the machined surface, and uppermost importance of the uncut chip thickness. Cutting speed is chosen at $V_c = 160$ m/min to limit heat input and be consistent with industrial production conditions. The two samples expose roughness $R_{z\ prod} = 0.8$ µm and $R_{z\ ploughing} = 16.4$ µm. According to (Bissey-Breton et al., 2011) and sum up in Table 1, these two samples should have an affected layer thickness $A_{t1} = 3.19$ µm and $A_{t2} = 23.3$ µm.

As a first approach, hardness could reveal the modified layer of material underneath the surface (Kermouche et al., 2016). Because of the expected affected layer thickness, nano-indentation analysis is a way to point out a modification of the microstructure and the mechanical properties. Fig. 16 shows the hardness analysis made on both selected samples. The hardness decreases from 160 HV in the bulk to 20 HV in the first 20 µm under the turned surface. Such a sharp and sudden decrease is not noticed in the literature and is more likely to be the resulting of an edge effect due to the analysis protocol and sample preparation. Because of the probe size of the nano-indenter, no meaningful measurement can be made close to the surface (<25 µm). However, it allows us to consider a limit with bulk material after 50 µm. Between 50 µm and 400 µm hardness stabilizes around the bulk hardness value 160 HV. Hence the nanoindentation technique is not suitable to analyze the first affected

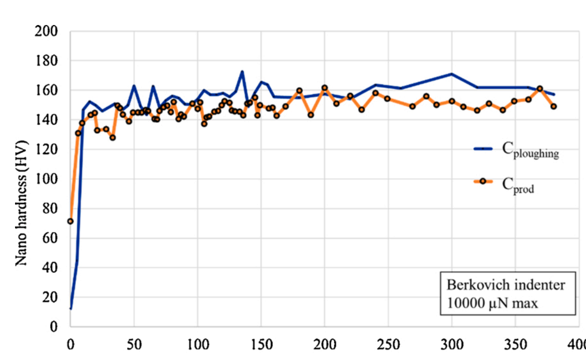

Fig. 16. Nanoindentation profile bellow the turned surface, for both cutting condition.

layer.

With a better resolution, EBSD allows the analysis of more information about the affected layer and its material structure. KAM criterion (Kernel Average Misorientation) can highlight the local disorientation linked to heterogeneity of dislocation density (Leaux, 2012). Fig. 17 is a comparison between an annealed pure copper and the bulk sample (half-hard 3D forged). While pure copper is completely blue and therefore perfectly homogeneous, the bulk material is crossed by green lines representing local disorientations related to the forging process.

Application of the KAM criterion is conducted in the sample C_{prod} visible in Fig. 18. Observation of the first 130 µm under surface reveals two different zones. Over 60 µm, green parallel lines, oriented in the same direction are visible distinctly. The structure in the grain is organized in localized deformation bands. This structure is the same in the bulk, already shown in the previous analysis. These microbands and this structure is representative of the material state before machining. The other zone, 0–60 µm, reveals a lower density of these bands. Dislocations are distributed homogeneously without an organized structure. In this zone, the material is affected by thermal flow induced by turning. Previous KAM analysis on an annealed material has confirmed this hypothesis by showing material with many micro bands structure. As for the nano-indentation measurement, an edge effect distorts the analysis of the first micro-meter.

To avoid the edge effect, FIB technology is commonly used for the preparation of high precision samples. By manufacturing a micrometric blade as illustrated on Fig. 19 directly under the machined surface, the first affected layer and the grains are preserved. Combined with a TEM observation, a 1.4 nm resolution is reached (against 200 nm with the previous EBSD).

By using these techniques, both samples show in the first 10 µm three different layers visible under the surface, as it is shown in Fig. 20:

A Recrystallized layer is made up of equiaxed grain with a diameter from 0.1 to 0.4 µm. The recrystallized thickness t_{rec} doubles with the ploughing condition. Grains boundaries are clearly visible. It is a clear indication that the thermo-mechanical flow created during the turning operation gives enough energy to activate the recrystallization process.

B Highly Elongated grains with deformed boundaries and a thickness between 0.2 µm to 0.6 µm for a length longer than 1 µm. This tends towards a thermo-mechanically affected layer. Under the force of the cutting process, the grains are elongated along with the surface, which could be sign of dragged material layer (la Monaca et al., 2021). The higher mechanically affected material is represented with a higher contrast of texture and allow measuring a deformed thickness t_{def}. Conditions are less intense than the previous layer. Grains are mechanically deformed, but the thermal flow is not high enough to initiate the recrystallization, hence annealing this layer.

C Due to the pyramidal shape of the sample, several grains are superimposed, and conclusions are limited. Material is affected by a marked internal texture, which is the image of the density of dislocation. This layer sees the tool action because it is not similar texture as the bulk, but the thermo-mechanical loading is not high enough to initiate major microstructural modification.

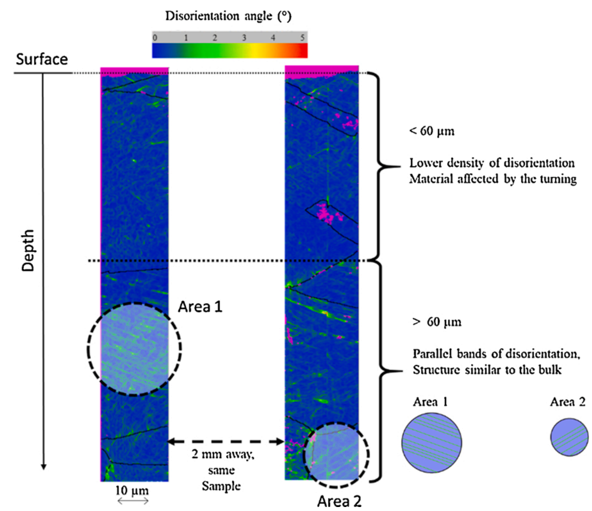

Fig. 18. EBSD KAM analysis of the C_{prod} sample in two areas.

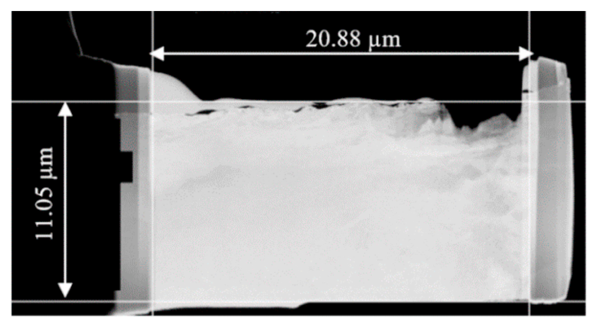

Fig. 19. Blade manufactured by FIB and used for TEM.

The highlighted structure shows the grain shape and boundaries. Hence the difference between layer A and B is clearly visible on the C_{prod} sample.

In case of ploughing condition (Fig. 21), structure A is two to three time thicker. Because of the higher internal texture in this case, boundaries are more difficult to observe, but structure B (elongated grain) extends far deeper in this case.

For both samples' conditions, the FIB-TEM analysis highlighted the microstructural modifications caused by the turning operation. The subsurface is modified with a recrystallized layer as well as a layer of deformed grains. The thickness of the layers was characterized by optical measurement. In the case of ploughing turning condition, the thickness of the affected layer (recrystallized and deformed grain) is three-time larger than that currently obtained with the production

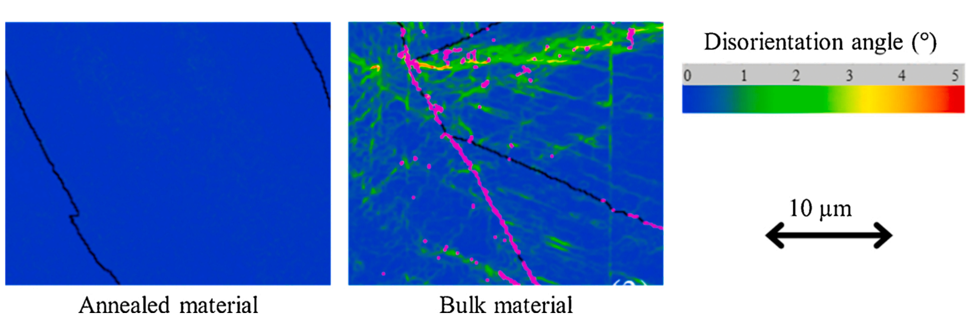

Fig. 17. Comparison of KAM criterion used on annealed, and 3D forged pure copper.

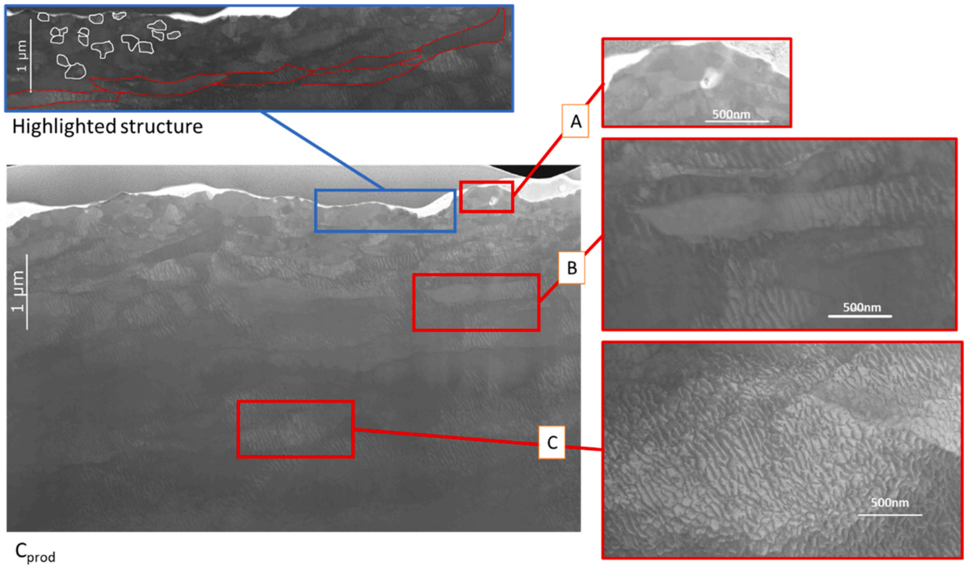

Fig. 20. TEM analysis of the production conditions blade made by FIB. Highlighting of the nano-grains (A), deformed grains (B) and dislocation texture (C).

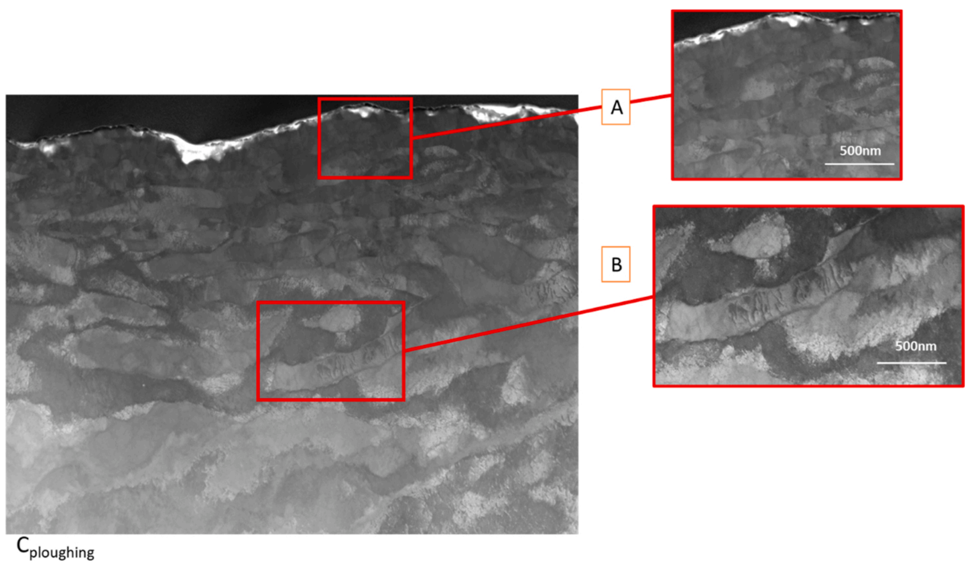

Fig. 21. TEM analysis of the ploughing condition sample blade made by FIB. Highlighting of the nano-grains (A), deformed grains (B).

condition, as detailed in Table 2. Moreover, if the cutting condition stays in an acceptable range of value, as defined in §3 and §4, the obtained subsurface is following literature results, both in term of texture and thickness of the affected layer. But, outside this window, ploughing phenomena leads to more intense sub-surface alteration, and diverge from theoretical behavior.

In case of superfinishing of pure copper, for a constant chip cross-section, it is preferable to use a low feed rate with a higher depth of cut. Therefore, the work material is less affected. With an affected thickness of around 4 µm for production condition, any other characterization process can distinguish nanoscopic size grains in these layers smaller than 3 µm and directly under the turned surface.

6. Conclusions

The pollution-free, demanding surface finish, turning operating presented in this study implies to work with alcohol-based lubrication while keeping cutting condition close to the minimal value for uncut chip thickness h_{eq}, chip cross-section A_d or cutting speed V_c. To limit the thickness of the affected layer, the chip cross-section must be minimized while keeping $h_{eq} > h_{eq(mini)}$, to avoid the ploughing phenomenon. This allows to limit the thermal and mechanical load, while keeping surface

Table 2
Summary of the thickness of the affected layer for the two samples of the study and comparison with estimation acc. (Bissey-Breton et al., 2011).

	C_{prod}		$C_{ploughing}$	
	This study	Estim. (Bissey-Breton et al., 2011).	This study	Estim. (Bissey-Breton et al., 2011).
t_{rec} (µm)	0.6	5	1.5	23
t_{def} (µm)	4		10	

integrity under control. Especially, it has be shown the prevalence of $h_{eq\ (mini)}$, both at macroscale (for cutting forces) and microscale (for microstructure modification). Conventional characterization methods EBSD and nano-hardness are quickly limited by edge effects and size of affected layers. Both samples have been produced to highlight the limit regime between cutting and ploughing, while keeping same A_d and V_c. Advanced microstructure technics like TEM and FIB have shown a subsurface of the turned OFE copper, in normal production condition, which is a succession of layer underneath the finish surface:

- Down to 0.6 μm, a completely recrystallized material, with ultra-fine grain structure.
- Between 0.6 μm and 4 μm, highly deformed grain, sign of thermo-mechanical load.
- Between 4 μm and 60 μm, a lower density of dislocation than the bulk.

In ploughing regime, the layers size is three time larger.

Keeping the cutting condition in a specific window of optimal parameters leads to reduce the affected layer and allows close control of the grain size. This work highlights the need of minimal cutting condition to ensure proper surface characteristics. The standard behavior of reducing feed rate or cutting speed to try to obtain proper surface finish is in contradiction of the present results. Maintaining sufficient uncut chip thickness is the primary factor driving the subsurface modification. This aspect has also been found in other application, such as corrosion resistance or fatigue, in aeronautic of energy field. Nevertheless, the present findings will serve as guideline for future production, in-house or subcontracted.

The main limiting factor in this study is the cleanliness of the operation through alcohol MQL as cutting fluid. The thermal balance cannot be fully estimated but this method is not sufficient to withstand high thermal input, such as higher cutting speed. Innovative cutting fluid such as CO2 would have to be investigated because it preserves the clean requirement, but vastly improve the thermal balance. It is confirmed by preliminary tests, and according to literature, surface integrity would be improved too. In case of corrosion sensitive application for copper, the reduce use of chemical compounds would be of great help to prevent basic copper carbonate or chloride quick appearance or limit the rate of propagation.

Grain topology is of paramount importance for the following process of niobium sputtering, as well as the crystal misorientation or even internal grain structure. It would be necessary to evaluate further if the produced microstructure is better for later grain growth during the coating process. Also, the alternative cutting condition could be used to compare the radio frequency performance of the produced cavities. Hence, these results should be compared to discontinuous cutting process such as milling, which is apply in case of more complex radio-frequency cavity shape.

CRediT authorship contribution statement

A. Camelin: Investigation, Resources, Data curation, Writing - original draft, Writing - review & editing, Visualization. **P. Naisson:** Supervision, Data curation, Writing - original draft, Writing - review & editing, Visualization. **G. Poulachon:** Conceptualization, Formal analysis, Supervision. **A. D'Acunto:** Conceptualization, Formal analysis, Supervision. **S. Atieh:** Conceptualization, Supervision.

Declaration of Competing Interest

The authors report no declarations of interest.

Acknowledgements

The author wants to thank Ana Teresa PEREZ FONTENLA and Dr. Floriane LEAUX for their expertise and a great help in EBSD and electron microscopy analysis.

References

AFNOR, 1997. NF E66-520-4: Domaine de fonctionnement des outils coupants–Couple outil-matière–Partie 4 : mode d'obtention du couple outil-matière en tournage.
Atmani, Z., Haddag, B., Nouari, M., Zenasni, M., 2015. Multi-physics modelling in machining OFHC copper – coupling of microstructure-based flow stress and grain refinement models. Procedia CIRP 31, 545–550. https://doi.org/10.1016/j.procir.2015.03.023.
Bellows, G., Tishler, D.N., 1970. Introduction to Surface Integrity.
Bissey-Breton, S., Gravier, J., Vignal, V., 2011. Impact of superfinish turning on surface integrity of pure copper. Procedia Eng. 19, 28–33. https://doi.org/10.1016/j.proeng.2011.11.075.
Cabanettes, F., Faverjon, P., Sova, A., Dumont, F., Rech, J., 2017. MQL machining: from mist generation to tribological behavior of different oils. Int. J. Adv. Manuf. Technol. Vol. 90, 1119–1130. https://doi.org/10.1007/s00170-016-9436-0.
Campocasso, S., Costes, J.-P., Fromentin, G., Bissey-Breton, S., Poulachon, G., 2015. A generalised geometrical model of turning operations for cutting force modelling using edge discretisation. Appl. Math. Model. 39, 6612–6630. https://doi.org/10.1016/j.apm.2015.02.008.
CERN, 2015. Technical Specification N° 2000 - Ed. 8. EDMS No: 790780: Oxygen-Free Electronic coppersheets - Cu-OFE.
Chae, J., Park, S.S., Freiheit, T., 2006. Investigation of micro-cutting operations. Int. J. Mach. Tools Manuf. 46, 313–332. https://doi.org/10.1016/j.ijmachtools.2005.05.015.
Denguir, L., Outeiro, J., Fromentin, G., Vignal, V., Besnard, R., 2014. Influence of cutting process mechanics on surface integrity and electrochemical behavior of OFHC copper. Procedia CIRP 13, 186–191. https://doi.org/10.1016/j.procir.2014.04.032.
Denguir, L., Outeiro, J.C., Fromentin, G., Vignal, V., Besnard, R., 2017. A physical-based constitutive model for surface integrity prediction in machining of OFHC copper. J. Mater. Process. Technol. 248, 143–160. https://doi.org/10.1016/j.jmatprotec.2017.05.009.
Denkena, B., Köhler, J., 2010. Consideration of the form of the undeformed section of cut in the calculation of machining forces. Mach. Sci. Technol. 14, 455–470. https://doi.org/10.1080/10910344.2010.533102.
Fraser, M.A., Kadi, Y., Bernardes, A.P., Blumenfeld, Y., Bravin, E., Calatroni, S., Catherall, R., Goddard, B., Parchet, D., Siesling, E., Venturini Delsolaro, W., Vandoni, G., Voulot, D., Williams, L.R., 2017. Status of the HIE-ISOLDE Project at CERN, p. 7. https://arxiv.org/abs/1707.05129.
Germain, D., Fromentin, G., Poulachon, G., Bissey-Breton, S., 2010. A force model for superfinish turning of pure copper with rounded edge tools at low feed rate. In: 8th International Conference High Speed Machining. 8–10th December 2010, Metz, France.
Ghosh, G., Sidpara, A., Bandyopadhyay, P.P., 2021. Experimental and theoretical investigation into surface roughness and residual stress in magnetorheological finishing of OFHC copper. J. Mater. Process. Technol. 228.
Gravier, J., 2009. Impact de l'usinage de superfinition sur la zone affectée par le procédé. Université de Bourgogne, Dijon.
Herbert, C.R.J., Kwong, J., Kong, M.C., Axinte, D.A., Hardy, M.C., Withers, P.J., 2012. An evaluation of the evolution of workpiece surface integrity in hole making operations for a nickel-based superalloy. J. Mater. Process. Technol. 212 (8).
Kermouche, G., Jacquet, G., Courbon, C., Rech, J., Zhang, Y., Chromik, R., 2016. Microstructure evolution induced by sliding-based surface thermomechanical treatments - application to pure copper. Mater. Sci. Forum 879, 915–920. https://doi.org/10.4028/www.scientific.net/MSF.879.915.
Klocke, F., Eisenblätter, G., 1997. Dry cutting. Ann. CIRP 46, 519–526.
Kupferinstitut, D., 2016. Technical Documentation Cu-c2.
la Monaca, A., Murray, J.W., Liao, Z., Speidel, A., Robles-Linares, J.A., Axinte, D.A., Hardy, M.C., Clare, A.T., 2021. Surface integrity in metal machining - Part II: functional performance. Int. J. Mach. Tools Manuf. 164.
Leaux, F., 2012. Relation entre microstructure et fatigue d'un acier ferritique utilisé dans l'industrie automobile: élaboration d'indicateurs d'endommagement. Ecole Nationale Supérieure de Chimie de Lille, Lille.
Lin, Z.C., Lo, S.P., 1997. Ultra-precision orthogonal cutting simulation for oxygen-free high-conductivity copper. J. Mater. Process. Technol. 65 (1–3), 281–291.
Liu, R., Salahshoor, M., Melkote, S.N., Marusich, T., 2015. A unified material model including dislocation drag and its application to simulation of orthogonal cutting of OFHC Copper. J. Mater. Process. Technol. 216, 328–338. https://doi.org/10.1016/j.jmatprotec.2014.09.021.
Mondelin, A., Claudin, C., Rech, J., Dumont, F., 2011. Effects of lubrication mode on friction and heat partition coefficients at the tool–work material interface in machining. Tribol. Trans. 54, 247–255. https://doi.org/10.1080/10402004.2010.538489.
Mondelin, A., Valiorgue, F., Rech, J., Coret, M., Feulvarch, E., 2013. Modeling of surface dynamic recrystallisation during the finish turning of the 15-5PH steel. Procedia {CIRP} 8, 311–315. https://doi.org/10.1016/j.procir.2013.06.108.
Naisson, P., Rech, J., Paris, H., 2013. Characterization of friction properties during machining of various stainless steels. Eng. Trans. 61 (4), 239–248. ISSN 2450-8071. Available at: https://et.ippt.gov.pl/index.php/et/article/view/5.
Ni, H., Alpas, A.T., 2003. Sub-micrometer structures generated during dry machining of copper. Mater. Sci. Eng. A 361, 338–349. https://doi.org/10.1016/S0921-5093(03)00530-6.

Rech, J., Hamdi, H., Valette, S., 2008. Machining - Fundamentals and Recent Advances Chap 3: Workpiece Surface Integrity. Springer, London. ISBN 9781848002135.
Sgobba, S., 2006. Materials for High Vacuum Technology, an Overview, p. 28. https://doi.org/10.5170/CERN-2007-003.117.
Sublet, A., Aviles Santillana, I., Bartova, B., Calatroni, S., Jecklin, N., Mondino, I., Therasse, M., Venturini Delsolaro, W., Zhang, P., Cantoni, M., 2014. Nb Coated HIE-ISOLDE QWR Superconducting Accelerating Cavities: From Process Development to Series Production WEPRI042, p. 3.
Valiorgue, F., Rech, J., Hamdi, H., Gilles, P., Bergheau, J.M., 2012. 3D modeling of residual stresses induced in finish turning of an AISI304L stainless steel. Int. J. Mach. Tools Manuf. 53, 77–90. https://doi.org/10.1016/j.ijmachtools.2011.09.011.